HHS Public Access

Author manuscript

J Mol Cell Cardiol. Author manuscript; available in PMC 2019 April 01.

Published in final edited form as:

J Mol Cell Cardiol. 2018 April ; 117: 88–99. doi:10.1016/j.yjmcc.2018.02.005.

Elevated 20-HETE in Metabolic Syndrome Regulates Arterial Stiffness and Systolic Hypertension via MMP12 Activation

Amanda Soler[1], **Ian Hunter**[1], **Gregory Joseph**[1], **Rebecca Hutcheson**[1], **Brenda Hutcheson**[1], **Jenny Yang**[1], **Frank Fan Zhang**[1], **Sachindra Raj Joshi**[1], **Chastity Bradford**[2], **Katherine H. Gotlinger**[1], **Rachana Maniyar**[1], **John R. Falck**[3], **Spencer Proctor**[4], **Michal Laniado Schwartzman**[1], **Sachin A. Gupte**[1], and **Petra Rocic**[1]

[1]Department of Pharmacology, New York Medical College, Valhalla, NY 10595

[2]Department of Biology, Tuskegee University, Tuskegee, AL 36088

[3]Department of Pharmacology, University of Texas Southwestern Medical Center, Dallas, TX 75390

[4]Metabolic and Cardiovascular Diseases Laboratory, Alberta Institute for Human Nutrition, University of Alberta, Edmonton, Alberta T6G 2E1, Canada

Abstract

Arterial stiffness plays a causal role in development of systolic hypertension. 20-hydroxyeicosatetraeonic acid (20-HETE), a cytochrome P450 (CYP450)-derived arachidonic acid metabolite, is known to be elevated in resistance arteries in hypertensive animal models and loosely associated with obesity in humans. However, the role of 20-HETE in the regulation of large artery remodeling in metabolic syndrome has not been investigated. We hypothesized that elevated 20-HETE in metabolic syndrome increases matrix metalloproteinase 12 (MMP12) activation leading to increased degradation of elastin, increased large artery stiffness and increased systolic blood pressure. 20-HETE production was increased ~7 fold in large, conduit arteries of metabolic syndrome (JCR:LA-cp, JCR) vs. normal Sprague-Dawley (SD) rats. This correlated with increased elastin degradation (~7 fold) and decreased arterial compliance (~75% JCR vs. SD). 20-HETE antagonists blocked elastin degradation in JCR rats concomitant with blocking MMP12 activation. 20-HETE antagonists normalized, and MMP12 inhibition (pharmacological and MMP12-shRNA-Lnv) significantly improved (~50% vs. untreated JCR) large artery compliance in JCR rats. 20-HETE antagonists also decreased systolic (182±3 mmHg JCR, 145±3 mmHg JCR+20-HETE antagonists) but not diastolic blood pressure in JCR rats. Whereas diastolic pressure was fully angiotensin II (Ang II)-dependent, systolic pressure was only partially Ang II-dependent, and large artery stiffness was Ang II-independent. Thus, 20-HETE-dependent

Corresponding Author: Petra Rocic, Ph.D., Department of Pharmacology, BSB 502, New York Medical College, 15 Dana Road, Valhalla, NY 10595, petra_rocic@nymc.edu, Phone: 914-594-4123; Fax: 914-347-4956.

DISCLOSURES

None.

regulation of systolic blood pressure may be a unique feature of metabolic syndrome related to high 20-HETE production in large, conduit arteries, which results in increased large artery stiffness and systolic blood pressure. These findings may have implications for management of systolic hypertension in patients with metabolic syndrome.

Keywords

20-HETE; MMP12; elastin; macrocirculation; arterial compliance; systolic hypertension

INTRODUCTION

Large artery stiffness is a major risk factor for hypertension, stroke and myocardial infarction [1]. Structural properties of large arteries, medial thickness and composition of the extracellular matrix (ECM), are the main determinants of large artery stiffness [2].

Despite the significant contribution of the ECM to increased blood pressure development and maintenance, no currently available anti-hypertensive therapy directly targets the ECM, although some (e.g. angiotensin converting enzyme inhibitors (ACEIs) and angiotensin receptor blockers (ARBs)) do affect it. Targeting elastin fiber integrity has been proposed as an effective therapy to specifically target systolic hypertension. Studies in elastin knockout mice have shown that its deficiency leads to a severe and fatal increase in systolic pressure, which is preceded by arterial stiffening, suggesting a causative role for elastin in maintenance of not only arterial compliance but also of normal systolic pressure [3].

Matrix metalloproteinase 12 (MMP12), one of the major elastin-degrading proteases, is secreted primarily from monocytes and neutrophils [4], but can also be made by synthetic vascular smooth muscle cells (VSMCs) [5]. Its upstream regulators are unknown. It has been implicated in chronic obstructive pulmonary disease and emphysema, atherosclerosis in type II diabetes, aneurysms, cancer and stiffening of femoral arteries in response to injury [5–9]. Its role in arterial stiffness in metabolic syndrome or hypertensive animals or humans has not been investigated. MMPs classically associated with the regulation of hypertension-induced arterial stiffness are MMP2 and MMP9, but their activity does not fully account for either large artery stiffness or systolic hypertension in animal models or humans [10].

20-hydroxyeicosatetraeonic acid (20-HETE) is synthesized from arachidonic acid by cytochrome P450 (CYP) [11]. In rats, CYP4A (A1, A2, A3, A8) and CYP4F (F1, F4) are the CYP isoforms which produce 20-HETE. 20-HETE is synthesized and released from many cell types including VSMCs [12], endothelial cells, neutrophils [13] and bone marrow cells [14].

The association with and causative role of 20-HETE in the development of hypertension is now well established. In the SHR rat, depletion of CYP4A decreased 20-HETE and significantly lowered mean arterial blood pressure [15]. Androgen-driven hypertension in mice and rats, the Cyp4a14 (−/−) androgen-dependent 20-HETE-mediated hypertension mouse model, the Cyp4a12 doxycycline inducible mouse model, and the Sprague-Dawley (SD) rat overexpressing CYP4A2 in the vascular endothelium exhibit increased 20-HETE

production and hypertension [16–19]. However, 20-HETE's role in the regulation of vascular structural remodeling is just emerging. Only recently, Schwartzman's group demonstrated that 20-HETE induced microvascular remodeling, which was only partially Ang II-dependent[20]. Furthermore, all previous studies evaluated the effect of 20-HETE manipulation only on mean arterial blood pressure (MABP). Moreover, because in normal, healthy animals 20-HETE is not produced in large arteries, all work focused on the role of small, resistance arteries and the contribution of myogenic tone to the regulation of systemic blood pressure. Therefore, nothing is known about the possible effect of 20-HETE in large arteries or on extracellular matrix (ECM) remodeling.

In this study, we explore a novel idea that, in the metabolic syndrome, 20-HETE specifically modulates systolic but not diastolic blood pressure, and that it does so by regulating large artery compliance, as a critical determinant of arterial stiffness, through regulating elastin degradation via MMP12 activation.

MATERIALS AND METHODS

Animals

10–12 week old, male JCR:LA-cp (JCR; S. Proctor, University of Alberta, Edmonton, Canada) (650–700g), spontaneously hypertensive obese (SHROB, Charles Rivers, Wilmington, MA) (650–700g) and Sprague-Dawley (SD; Charles Rivers) (300–350g) rats were used in all experiments. The JCR rat is a cross between the lean LA/N Zucker and the spontaneously hypertensive obese (SHROB) rat developed in the laboratory of Dr. Carl Hansen at the National Institutes of Health and sent to Drs. James C. Russell and Spencer Proctor (University of Alberta). By 8 weeks of age, the JCR rats develop obesity with fatty liver, and secondary to obesity, additional characteristic of metabolic syndrome: hypertension, insulin resistance with glucose intolerance, and complex dyslipidemia (low HDL, high LDL and vLDL). Unique to rodent models of metabolic syndrome, by 10 weeks of age, JCR rats develop severe vasculopathy characterized by decreased endothelium-dependent and - independent vasorelaxation, increased stiffness of large, conduit arteries [21], neointimal hyperplasia and intimal lesions morphologically identical to early atherosclerotic lesions in humans, as well as left ventricular hypertrophy and myocardial and cerebral (micro)infarctions. At 16+ weeks, the rats become prone to stroke and myocardial infarction, and at 18+ weeks, they develop he art failure[22,23]. Like the development of the metabolic syndrome and cardiovascular disease in humans, the apparent complexity of the cardio-metabolic phenotype exhibited by the JCR rats is suspected to be multifactorial and polygenetic in etiology, but the hypertensive component may significantly contribute to the overt cardiovascular pathology observed in this model. The SHROB rats are a parent strain to the JCR rats, and, at 10–12 weeks of age, are obese, hypertensive and insulin-resistant with glucose intolerance and complex dyslipidemia.

All experiments involving animals were performed in accordance with the Animal Welfare Act and are approved by the IACUC of New York Medical College.

20-HETE antagonists, AT1R blockade and MMP12 inhibition

JCR rats were treated with 20-HETE antagonists, losartan (Ang II type I receptor blocker (ARB)), calcium channel blocker (CCB, diltiazem chloride) or MMP12 inhibitors for 14 days starting at 10–12 weeks of age.

20-HETE antagonists—20-SOLA, [2,5,8,11,14,17-hexaoxanonadecan-19-yl 20-hydroxyicosa-6(z),15(z)-dienoate], was administered in drinking water at 10 mg/kg/day and 20-HEDGE, *N*-[20-hydroxyeicosa-6(*Z*),15(*Z*)-dienoyl] glycine, was administered via intraperitoneal injection (i.p.) at 10 mg/kg/day[19,24].

Losartan—Losartan monopotassium salt (2-Butyl-4-chloro-1-{[2′-(1*H*-tetrazol-5-yl)(1,1′-biphenyl)-4-yl]methyl}-1*H*-imidazole-5-methanol monopotassium salt) (Sigma-Aldrich, St. Louis, MO) was administered in drinking water at 3 mg/kg/day.

Diltiazem chloride—Diltiazem hydrochloride (Sigma-Aldrich) was administered in drinking water at 100 mg/kg/day.

MMP12 inhibition—MMP408, (S)-2-(8-(Methoxycarbonylamino) dibenzo(b-d)furan-3-sulfonamido)-3-methylbutanoic acid (Millipore, San Diego, CA), was administered i.p. at 3.5 mg/kg/day. We have previously shown that, at this dose used *in vivo*, MMP408 specifically inhibits >90% of MMP12 activation without affecting activity of other MMPs[25]. MMP12 shRNA lentiviral construct (MMP12-shRNA-Lnv) was from Thermo Fisher Scientific, Lafayette, CO. A non-targeting shRNA in an identical Lnv construct was used as control (control-Lnv). Lnvs were delivered at 10 μl of 1×10^8 transduction units/ml (TU/ml) stock in isotonic saline (100μL) by direct injection into the left ventricular cavity as described previously for lentiviral adenoviral vectors[26,27].

Liquid chromatography-tandem mass spectrometry (LC/MS/MS)

Arterial tissue (carotid arteries and thoracic aorta) was isolated and incubated in oxygenated Krebs bicarbonate buffer, pH 7.4, with 1 mM NADPH for 1 h at 37°C. The reaction was stopped by addition of 100% methanol and stored in −80°C overnight. Samples were vortexed and centrifuged for 5 min at 2000 rpm. The liquid phase was removed and tissue dried and used for protein concentration measurements. The Department of Pharmacology Mass Spectroscopy Core Facility performed 20-HETE and epoxyeicosatrienoic acids (EETs) analysis using LC/MS/MS spectrometry as previously described[28,29].

Western blotting

Arterial tissue (carotid arteries and thoracic aorta) was collected and snap-frozen in liquid nitrogen before homogenization in modified RIPA lysis buffer containing 1% SDS and 1% Triton. For collagen extraction, tissue was first subjected to acid hydrolysis with 6N HCl at 100°C for 72 hours, then homogenized in RIPA lysis buffer containing 1% SDS and 1% Triton. Equal amounts of protein were separated by SDS-PAGE and transferred to Trans-Blot® Turbo™ Mini-size PVDF membranes (Biorad, Hercules, CA). Primary anti-CYP4A1 (1:200, Santa Cruz, Dallas, TX), anti-MMP12 (1:250, Santa Cruz, Dallas, TX), anti-MMP2 and -MMP9 (1:1000, Millipore, Temecula, CA), anti-MMP3, -MMP7 and – MT1-MMP

(1:1000, Abcam, Cambridge, MA), anti-TIMP1, -TIMP2, -TIMP3 and – TIMP4 (1:1000, Abcam), anti-collagen I and – collagen III (1:1,000, Abcam), and anti-elastin (1:200, Santa Cruz, sc-58756, recognizes intact elastin and degradation products) and secondary anti-rabbit or anti-mouse antibodies (BioRad), as appropriate, were used for Western blotting. Bands were visualized by the Odyssey Western blot detection system (Azure Biosystems, Dublin, CA). Bands were quantified using Un-Scan-It Image software (Silk Scientific Corporation, Orem, UT). Data are normalized to β-tubulin (loading control).

Immunohistochemistry (IHC)

Arterial tissue (carotid arteries and thoracic aorta) mounted in Optimal Cutting Temperature (OCT) blocks was cut into 10μm sections. Primary anti-elastin (1:200, Santa Cruz, sc-166543, recognizes only intact elastin) and secondary AlexaFluor594-conjugated (Sigma-Aldrich) antibodies were used. Verhoeff–Van Gieson stain (VVG) was also used to detect elastin. Red (Alexa594) fluorescence or bright-field representative images were collected using a Zeiss fluorescent microscope equipped with Zeiss software.

Pressure myography

Freshly isolated carotid arteries (~400μM internal diameter) and thoracic aorta (~1,000μM internal diameter) were mounted on cannulas in a pressure myograph system (JP Trading, Aarhus, Denmark) and equilibrated for 1 hour in Ca^{2+}-free oxygenated Kreb's Buffer at 37°C. A passive pressure-diameter curve was generated by increasing intraluminal pressure stepwise from 4 to 140 mmHg, and wall thickness (WT) and internal diameters (Di) were recorded at each pressure. Aortas were perfused with tetrazolium blue chloride (Sigma-Aldrich) to allow for reliable demarcation of the arterial wall. This range of pressures encompasses the physiological range of mean arterial pressure (MAP) in SD, JCR and SHROB animals. Vessel diameters were plotted in response to increasing intravascular pressure as an index of arterial stiffness. For measurements of axial stretch only, vessel segments were attached to movable cannulas connected to a micrometer, and longitudinal segment length was measured at 4 mmHg and MAP (95 mmHg for SD and 152 mmHg for JCR). Axial stretch is reported as the ratio of length at MAP/length at 4 mmHg.

Blood pressure measurements

SD, JCR and SHROB rats were anesthetized with 2% Isoflurane and PE-50 catheter filled with heparin (10 U/mL)-saline was inserted into the common carotid artery and advanced into the ascending aorta, secured and externalized between the scapulae 3 days before onset of treatment as described previously [30]. The catheter was connected to a micromanometer (Millar Instruments, Houston, TX), and systolic and diastolic blood pressure measured at time of surgery, at the beginning of treatment (day 3 post surgery = day 0 of treatment), middle (day 7), and end of treatment (day 14) in rats lightly anesthetized with 2% Isoflurane.

Echocardiography

Echocardiography was performed as described previously [21,31]. All measurements were performed under Isoflurane (1–2%) anesthesia with continuous monitoring of body temperature, blood pressure and heart rate. Left ventricular end-diastolic diameter (LVEDD)

and end-systolic diameter (LVESD), septal wall diastolic thickness (IVSWT) and left ventricular free (posterior) wall diastolic thickness (LVWT) were measured by 2D guided M-mode echocardiography from the parasternal long-axis view by using a 12–38 MHz vascular probe (Vevo 770, 1,000 fps, Visual Sonics, Toronto, Ontario, Canada). Left ventricular end diastolic and systolic volumes (LVEDV and LVESV) and ejection fraction (EF) were calculated using Vevo software (Visual Sonics).

Statistical analysis

All experiments were n=8 animals per treatment group. Results were analyzed by two-way ANOVA followed by Bonferroni correction. $p<0.05$ determined statistical significance.

RESULTS

CYP4A, CYP4F and 20-HETE are elevated in metabolic syndrome

CYP4A (4A1, 2, 3 and 8) and CYP4F (4F1 and 4) are the CYP isoforms expressed in rat which make 20-HETE; the rat expresses 4F5 and 6 but these two isoforms do not make 20-HETE[32]. Our results indicate that CYP4A and CYP4F are expressed in carotid arteries and aorta of JCR and SHROB but not of SD rats (~2 fold JCR vs. SD) (Figure 1A and Figure VIII, Supplement). By RT-PCR analysis, we have identified the CYP4A isoforms expressed in arteries of JCR and SD rats to be 4A2 and 4A3; whereas, 4A1 expression is minimal and 4A8 expression undetectable (Figure IA, Supplement). Both the 4F1 and 4F4 isoforms are expressed in large arteries of SD and JCR rats (Figure IB, Supplement).

Increased CYP4A/4F expression correlated with increased 20-HETE production in large arteries of JCR vs. SD rats (~7 fold) (Figure 1B). Importantly, like all large, conduit arteries examined in previous studies [33], carotid arteries and aorta in this study in normal animals do not express significant amounts of CYP4A/4F, but the metabolic syndrome phenotype induces their expression in these arteries (Figure 1). Notably CYP4F, which is expressed in leukocytes in rats and humans [34,35], was expressed at a slightly lower level in the aorta vs. carotid arteries; whereas, CYP4A, which is thought to be expressed in VSMCs [36], was expressed equally in both vascular beds (Figure 1A). This resulted in ~25% lower 20-HETE production in aorta vs. carotid arteries.

14,15-EETs and 11,12-EETs were significantly decreased in the aorta and carotid arteries of JCR vs. SD rats, but 14,15-EETs, 11,12-EETs, 8,9-EETs or 5,6-EETs were not altered by 20-HETE antagonists in our studies (Table 1, Supplement). There was no significant difference in EET levels between aorta and carotid arteries (Table 1, Supplement). Also, in agreement with previous studies [37], production of these EETs was lower in large conduit arteries, which are the focus of this study, vs. resistance arteries (small mesenteric or coronary arteries) (Table 1, Supplement).

20-HETE induces MMP12 activation and elastin degradation in metabolic syndrome

Correlating with increased 20-HETE production, our results further demonstrate that MMP12 activation is significantly increased in large systemic arteries of metabolic

syndrome (JCR) animals (~2 fold vs. SD) (Figure 2A). There was no difference in the absolute or relative magnitude of MMP12 activation between the two vascular beds.

Increased MMP12 activation, in turn, correlated with increased degradation of elastin as shown by disappearance of the 68kDa band corresponding to intact elastin and appearance of the 45 kDa band corresponding to an elastin degradation product generated by cleavage by MMP12 on Western blot in JCR but not in SD rats (Figure 2B). This was further confirmed by immunohistochemistry using anti-elastin antibodies or the elastin-specific VVG stain which demonstrate decreased intensity of staining within the vascular wall between the internal and external elastin lamina in carotid arteries and aorta (Figure 2C), which appears to be a result of increased fragmentation of elastin fibers within the vascular wall, between the laminae (Figure 2D and Figure II, Supplement).

Total elastin content increased with increasing size of the artery, while the amount of degraded elastin and relative % of degraded elastin decreased (Figure 2B). Since MMP12 activation was the same in both vascular beds, these results are likely a consequence of vessel morphology, i.e. increasing amounts of elastin with increasing vessel diameter and wall thickness.

Upstream regulators of MMP12 activation in the cardiovascular system are unknown. Our results demonstrate that 20-HETE induces MMP12 activation and elastin degradation in large arteries in metabolic syndrome since the 20-HETE antagonist, 20-HEDGE, administered at the dose of 10 mg/kg/day, which has been shown to lower blood pressure in our previous studies [38,39], completely blocked MMP12 activation and elastin degradation (Figure 2) in large arteries of JCR rats. This effect is Ang II-independent; losartan had no effect on elastin degradation (Figure 2C, 2D and Figure 2, Supplement) or on MMP12 activation (Figure 2A).

Similarly, the Ca^{2+} channel inhibitor (CCB), diltiazem chloride, which reduced systolic blood pressure in JCR rats to levels comparable to those achieved with 20-HETE antagonists (Figure IIIA, Supplement), had no effect on MMP12 activation or elastin degradation (Figure IIIC, Supplement).

MMP2 expression was higher in SD vs. JCR rats and was increased by 20-HETE antagonists; however, its activation was not different between SD and JCR rats and was not affected by the 20-HETE antagonist in the aorta (Figure IVA, Supplement). Neither expression nor activation of MMP9 was different between SD vs. JCR rats or in response to the 20-HETE antagonist in any of the large arteries examined. MMP7 was not expressed, and MMP3 was not active is the aorta of either rat phenotype (Figure IVA, Supplement). Identical results were obtained from carotid arteries.

Tissue inhibitors of matrix metalloproteinases (TIMPs) did not contribute to the 20-HETE-dependent regulation of MMP12 activity. TIMP2 expression was decreased in metabolic syndrome animals, but this decrease was not effected by 20-HETE antagonists or losartan (Figure IVB, Supplement). Interestingly, a higher molecular weight (~160 kDa) band which stained positively for TIMP2, was regulated by 20-HETE but not by Ang II, similarly to arterial stiffness. This large molecular weight band was identified as a complex between

TIMP2, inactive MMP2 and inactive MT1-MMP (also known as MMP14), which is known to form in VSMCs [40]. MT1-MMP is a collagenase, and thus, cannot directly regulate elastin degradation. However, since collagen was regulated in a 20-HETE-dependent manner (Figure V, Supplement), we investigated whether MT1-MMP activation was regulated by 20-HETE. Like MMP2, its expression was lower in JCR vs. SD rats and restored by 20-HETE antagonists, but it was not activated in either SD or JCR rats or in response to 20-HETE antagonism or AT1R inhibition (Figure IVB, Supplement). TIMP1 was detected only in a higher molecular weight (~110 kDa) complex with MMP9 [41], with a similar pattern of regulation as the TIMP2-MMP2-MMP14 complex (Figure IVC, Supplement). MMP9 is not differentially activated in normal vs. metabolic syndrome rats, nor is it regulated by 20-HETE (Figure IVA, Supplement); therefore, we conclude that the expression pattern of this complex band reflects expression of TIMP1 itself. In support of these results, treatment with candesartan did not alter TIMP1 expression in hypertensive patients [42].

MMP12 was not a part of either complex, as neither the TIMP2-nor the TIMP-1-containing high molecular weight band stained positively for MMP12 nor did either of the TIMPs co-immunoprecipitate with MMP12 (data not shown). Thus, neither of the TIMPs, which have been shown to be expressed in the cardiovascular system and putatively regulate MMP12, regulate its activity in our experiments.

TIMP3 expression was decreased in JCR vs. SD rats (expression in aorta was greater than in carotids) in accordance with previously published results [43], but was not regulated by either 20-HETE antagonists or AT1R blockers, and TIMP4 was not expressed in any of the blood vessels examined (Figure IVD, Supplement).

20-HETE regulates type I and type III collagen content in metabolic syndrome

Type I (70–80%) and type III collagen (~10%) comprise 80–90% of collagen in the vascular wall of normal vessels, the rest being type IV and V collagen, and their ratio is responsible for determining arterial stiffness [44]. Not surprisingly, type III collagen was significantly increased (~4 fold) and type I collagen significantly decreased (~50%) in JCR animals (Figure V, Supplement), correlating with increased stiffness. Losartan decreased type III collagen content, but did not affect collagen I expression or degradation. 20-HETE inhibition decreased collagen III content and increased collagen I content, but it also increased collagen I degradation.

This effect was not MMP12-dependent. As expected, MMP12 inhibition had no effect on collagen expression or degradation (Figure V, Supplement), since neither collagen I nor III are its substrates.

20-HETE is a major regulator to decreased arterial compliance in metabolic syndrome

Because elastin content and integrity are major determinants of arterial elasticity/stiffness, we next evaluated parameters of arterial compliance in the aorta and carotid arteries in JCR and SD rats (Figure 3). Arterial compliance was significantly decreased in JCR vs. SD rats as evident by a decrease in change in arterial diameter in response to increasing pressure (Figure 3A). Also, axial stretch was decreased for these arteries (1.67±0.02 JCR vs. 1.82±0.02 SD for aorta, 1.36±0.02 JCR vs. 1.44±0.02 SD for carotid arteries).

20-HEDGE as well as the water-soluble 20-HETE antagonist, 20-SOLA, restored the arterial compliance of carotid arteries and aorta in metabolic syndrome animals to that seen in normal (SD) animals (Figure 3A); thus, implicating 20-HETE as a major regulator of arterial stiffness in metabolic syndrome. Nearly identical results were obtained in SHROB rats (Figure VIII, Supplement). Axial stretch was similarly affected (1.91±0.01 JCR+20-HEDGE, 1.92±0.01 JCR+20-SOLA for aorta, 1.68±0.01 JCR+20-HEDGE, 1.69±0.03 JCR +20-SOLA for carotid arteries). In contrast, an angiotensin type I receptor blocker (ARB), losartan, did not significantly increase luminal diameter or wall thickness in response to increasing pressure (Figure 3A). Thus, AT1 receptor blockade did not significantly affect the overall stiffness/elasticity profile or axial stretch (1.76±0.01 JCR for aorta, 1.59±0.02 JCR for carotid arteries) in JCR rats. These results indicate that arterial stiffness in the JCR rats is 20-HETE-but not Ang II-dependent. 20-HETE antagonists impacted (increased) internal diameter (Figure 3A) but did not significantly alter wall thickness (Figure 3B). In contrast to ARBs, which have been shown to attenuate medial thickening (VSMC hypertrophy) in hypertensive animal models but did not have marked effects on arterial compliance [45–47], our results indicate that 20-HETE antagonists specifically target arterial compliance, which largely depends on structural elastic properties of vessels.

Diltiazem chloride, a CCB, did not affect arterial stiffness, either lumen diameter or wall thickness in the aorta (Figure IIID, Supplement), indicating that the effect of 20-HETE antagonists on arterial compliance is blood pressure-independent. Axial stretch was similarly unaffected.

MMP12 is an important but not the sole regulator of elastin degradation in metabolic syndrome

Since 20-HETE antagonists completely blocked MMP12 activation and elastin degradation in the JCR rat model of metabolic syndrome, we next wanted to determine whether MMP12 was a major protease responsible for increased elastin degradation in metabolic syndrome.

Results in Figure 4 demonstrate that elastin degradation in metabolic syndrome is primarily, but not solely, MMP12-dependent since MMP12 inhibition by a specific pharmacological inhibitor (MMP408, administered at the dose of 3.5 mg/kg/day, which has been shown to inhibit ~90% of MMP12 activation without affecting activation of other MMPs in our previous study [48], and by an MMP-12 shRNA (MMP12-shRNA-Lnv) resulted in ~50% decrease in elastin degradation (vs. JCR). The incomplete inhibition of elastin degradation was not due to partial inhibition of MMP12 activity by MMP408 or MMP12-shRNA-Lnv, which resulted in ~90% and ~100% inhibition of the increase in MMP12 activation, respectively (Figure VIA, Supplement).

MMP12 is partially responsible for reduction in arterial compliance in metabolic syndrome

Similarly, both the specific MMP12 pharmacological inhibitor (MMP408) and the MMP12-shRNA-Lnv partially restored elasticity of the large arteries in JCR rats (Figure 5) and axial stretch (1.86±0.01 JCR+MMP408, 1.86±0.02 JCR+MMP12-shRNA-Lnv for aorta, 1.61±0.02 JCR+MMP408, 1.60±0.03 JCR+MMP12-shRNA-Lnv for carotid arteries), not surprisingly indicating that, as with degradation of elastin which was also incompletely

inhibited by MMP12 inhibition (Figure 4), additional pathways regulate arterial elasticity/stiffness. MMP12 inhibitors significantly affected luminal diameter (Figure 5A), but not wall thickness (Figure 5B) indicating that, like 20-HETE antagonists, they act primarily on structural properties of the vessel which exclude wall thickness, such as the elastic properties of the arteries.

Neither MMP408 nor MMP12-shRNA-Lnv decreased 20-HETE levels (Figure VIB, Supplement), confirming that MMP12 activation is indeed downstream of 20-HETE.

20-HETE regulates systolic but not diastolic blood pressure in metabolic syndrome

JCR rats are hypertensive with elevated systolic (182±3 mmHg JCR vs. 110±6 mmHg SD) (Figure 6A) and diastolic (123±4 mmHg JCR vs. 80±6 mmHg SD) (Figure 6B) blood pressure. Both 20-SOLA and 20-HEDGE significantly decreased systolic blood pressure in JCR rats, to 145±3 mmHg and 149±2 mmHg, respectively, but did not affect diastolic blood pressure (120±3 mmHg JCR+20-SOLA and 124±2 mmHg JCR+20-HEDGE). Similar results were seen in SHROB rats (Figure VIII, Supplement).

Heart rate (HR) is not different between SD and JCR rats. Cardiac output (CO) is decreased in JCR rats (as a function of hypertrophic ventricular remodeling), but it is not affected by 20-HEDGE or 20-SOLA (Table 2, Supplement); thus, the observed effect of 20-HETE antagonists on systolic blood pressure solely reflects a difference in total peripheral resistance.

Losartan decreased both systolic (168±3 mmHg JCR+losartan vs. 182±3 mmHg JCR) and diastolic (78±4 mmHg JCR+losartan vs. 123±4 mmHg JCR) blood pressure (Figure 6). Of note, the effect of the ARB on systolic blood pressure was lesser than that of 20-HETE antagonists. These results indicate that a component of systolic hypertension in the JCR rat is 20-HETE-dependent but Ang II-independent and are consistent with results in Figure 3 which demonstrate that arterial stiffness, a major determinant of systolic hypertension, is also 20-HETE-dependent but Ang II-independent.

MMP12 inhibition, in accordance with partial reversal of elastin degradation and partial restoration of large artery compliance, resulted in significant but smaller improvement in systolic blood pressure in JCR rats (Figure VII, Supplement).

DISCUSSION

The most important findings in this study are: 1) that 20-HETE is highly elevated in large, conduit arteries of metabolic syndrome animals which correlates with increased elastin degradation, decreased large artery compliance and increased blood pressure in these animals, and 2) that 20-HETE antagonism reverses elastin degradation, restores large artery compliance and normalizes systolic but not diastolic blood pressure in the metabolic syndrome animals, and 3) that this effect is in part Ang II-independent since an ARB, losartan, had no effect on arterial compliance and its effect on systolic blood pressure was lesser than that of 20-HETE antagonists. Thus, our results indicate that 20-HETE is an Ang II-independent regulator of large artery elasticity and, in part, of systolic but not diastolic

blood pressure in metabolic syndrome. Furthermore, the effect of 20-HETE antagonists on arterial stiffness is blood pressure-independent since equivalent reduction in systolic blood pressure using a CCB had no effect on arterial elasticity.

Large artery stiffness is likely the single most important determinant of isolated systolic hypertension. It has been shown that systolic blood pressure is independently associated with pulse-wave velocity (PWV), which is a direct measure of large artery stiffness. Furthermore, PWV is increased even at the very early stages of hypertension, suggesting that it may be a causal factor. In turn, passive stiffening of large arteries is controlled predominantly by the extracellular matrix (ECM) components in the arterial wall, specifically by the balance between collagen and elastin synthesis and degradation as well as by collagen cross-linking. Elastin degradation was associated with progressive aortic stiffening in humans [49], and increased elastin degradation has been reported to lead to stiffer vessels, decreased compliance and increased arterial stiffness [3]. Elastin's particular contribution to regulation of arterial stiffness and blood pressure can be inferred from elastin knockout (*Eln*−/−) mice, which die within a few days of birth. At E18, left ventricular (LV) systolic blood pressures between *Eln*−/− and wild-type mice are similar. However, even at this early stage, incremental arterial stiffness is significantly elevated in *Eln*−/− mice. By post-natal day one, aortic stiffness is markedly increased and LV pressure in *Eln*−/− mice is double that of wild-type. Hence, increases in arterial stiffness precede changes in blood pressure, and elastin plays a crucial role in determining both [3].

Thus, maintaining total elastin content and its integrity is of paramount importance to maintaining vascular elasticity and normal blood pressure. In our study, 20-HETE antagonism but not blockade of Ang II signaling (ARB) reversed arterial stiffening in JCR rats. Losartan likewise failed to block elastin degradation in JCR rats. These results may seem somewhat surprising. ARBs and ACEIs have been show to decrease elastin degradation in aortic aneurysms [50]. However, their effect on ECM remodeling, especially with respect to elastin degradation, appears to be far lesser within the context of arterial stiffness. Telmisartan only partially reduced elastin degradation in a rat model of STZ-induce diabetes [51]. In SHR rats, Ibesartan somewhat improved the collagen/elastin ratio, but mostly through decreasing collagen synthesis [52]. In another study, treatment with ACEIs reversed medial thickness without changing the absolute amount of elastin [53]. Moreover, chronic ACEI treatment only slightly increased basal carotid compliance and did not change carotid compliance when VSMC contraction was inhibited, indicating that ACEIs have no effect on the ECM-dependent component of compliance/stiffness [51]. Another study showed that in SHR rats only early treatment with an ACEI, before any significant increase in arterial stiffness or blood pressure (6–10 weeks of age), effectively, although still only partially, modifies the ECM of the arterial wall and reduces loss of arterial compliance, whereas late treatment (20–24 weeks) is ineffective [55]. Thus, overall, ACEIs and ARBs are largely ineffective at reversing elastin degradation and established arterial stiffness, which is in agreement with results in our present study.

This highlights the significance of 20-HETE antagonists' ability to completely reverse elastin degradation and restore arterial compliance in the metabolic syndrome animals to that seen in normal, healthy animals. The mechanism for the differential effect of ACEIs/

ARBs and 20-HETE antagonists is unknown. Our study demonstrates that part of the reason may lie in their differential effect on MMP12-induced elastin degradation. A study has shown that MMP12 activation induced by vascular injury resulted in increased arterial stiffness, which was not mediated by vascular smooth muscle remodeling or reactivity, but by the microenvironment [5].

In addition, 20-HETE antagonists were able to completely revert the pattern of collagen expression in metabolic syndrome animals to that seen in normal animals, while ARBs decreased type III collagen, but failed to increase intact type I collagen or decrease its degradation. Since increased collagen III and decreased collagen I content have been correlated with increased stiffness [56–58], the observed restoration of arterial compliance by 20-HETE antagonists may also be in part mediated by their effect on collagen turnover. Collagen crosslinking by advanced glycation end products (AGEs) is another important predictor of stiffness [59]. AGE formation is increased by hyperglycemia, oxidative stress and Ang II [59], which are elevated in JCR rats and human metabolic syndrome patients. Thus, it is likely that AGE-mediated collagen crosslinking also significantly contributes to large artery stiffness in JCR rats. This and additional extracellular matrix alterations which might contribute to stiffness and systolic hypertension will be evaluated in future studies.

Furthermore, while ARBs and ACEIs decreased both systolic and diastolic blood pressure, 20-HETE antagonists specifically lowered only systolic blood pressure. Isolated systolic hypertension is particularly difficult to manage due to currently available antihypertensive drugs' equal effect on both systolic and diastolic blood pressure, and consequential lowering of diastolic blood pressure to excessively low levels resulting in symptomatic organ hypoperfusion, or inadequate lowering of systolic blood pressure. Elevated systolic blood pressure is a major determinant of end organ damage. Thus, identifying a mechanism that can be manipulated by pharmacological therapy, so that it specifically targets systolic but not diastolic blood pressure, would be highly beneficial.

20-HETE and Ang II interaction has been linked to hypertension. 20-HETE activates the Ras/MAPK pathway [60] to mediate Ang II-dependent vasoconstriction and mitogenic effects associated with hypertrophy and hypertension [60–64]. In human and rat microvascular endothelial cells, 20-HETE potently induces transcriptional activators of endothelial ACE, thus increasing conversion of angiotensin I to Ang II for potentiation of Ang II actions [28,65]. Vice versa, Ang II has been shown to stimulate 20-HETE synthesis and release in rat preglomerular microvessels further contributing to Ang II-mediated pressor effects [66–68]. Further studies demonstrated that upon 20-HETE inhibition, the Ang II renal pressor response leading to Ang II-dependent hypertension was attenuated [66,69]. Therefore, in the aggregate, with respect to blood pressure regulation, 20-HETE and Ang II appear to jointly regulate myogenic tone, the component of blood pressure regulation provided by the small, resistance arteries. However, there is no evidence that 20-HETE and Ang II interact in the regulation of large artery diameter. Thus, control of large artery diameter via compliance/stiffness may be mainly 20-HETE-dependent, at least in metabolic syndrome.

20-HETE has been associated with hypertension via regulation of increased peripheral resistance. However, these studies were not conducted in obese or metabolic syndrome animals [11,70,71]. The CYP isoforms which produce 20-HETE are not expressed in large arteries in normal animals (in agreement with results with our study), but only in the smaller resistance arteries [33], which likely accounts for the effect of 20-HETE on systemic blood pressure which is mediated through increase in peripheral resistance, i.e. vasoconstriction of small arteries, in these animal models. In contrast, our study demonstrates that in the metabolic syndrome animals, large arteries, including the aorta and carotid, express high levels of these enzymes and exhibit high 20-HETE production. It is possible that 20-HETE-dependent regulation of systolic blood pressure is a unique feature of metabolic syndrome (and perhaps obesity and/or obesity-induced type II diabetes) related to high CYP4A and CYP4F expression and resultant high 20-HETE production in large arteries of these animals; ultimately, resulting in increased large artery stiffness -a primary determinant of systolic blood pressure.

On the other hand, highly elevated systemic 20-HETE levels have been demonstrated in fructose-fed, obese and insulin-resistant rats [72], as well as in human metabolic syndrome patients [73]. Although, regulation of the CYP enzyme isoforms, which produce 20-HETE, by Ang II has not been extensively studied in tissues other than the vasculature, one study showed that Enalapril reversed induction of the 20-HETE CYP synthase in the kidney of high-fat-fed mice [74]. A single study also reported that Ang II induced 20-HETE release from renal microvessels ex-vivo via AT2 receptors and phospholipase C [75].

In this study, we also did not investigate additional upstream regulators of 20-HETE production in metabolic syndrome, including the possible contribution of cellular metabolism and its by-products on 20-HETE-mediated modulation of arterial stiffness or blood pressure. Elevated superoxide ($O_2^{\cdot -}$) levels and resultant decrease in nitric oxide ($NO^{\cdot -}$) bioavailability, which are a known feature of the vasculature in metabolic syndrome, including in the JCR rats [21,76], have been associated with elevated 20-HETE levels [21,77,78]. We hypothesize that CYP4F expression may be increased in large part due to increased adhesion and prolonged survival of neutrophils, which we observed in coronary arteries of JCR rats [35], a consequence of endothelial dysfunction [35], and the synthetic VSMC phenotype [79,80].

Lipoprotein-associated PLA_2 is also elevated in patients with metabolic syndrome and predicts cardiovascular disease [81,82]. Thus, it seems reasonable to hypothesize that PLA_2 is likewise elevated in JCR rats resulting in freer arachidonic acid (AA). Another factor determining the amount of free AA available for conversion to 20-HETE by CYP4A/4F is how much of it is used by COX and LOX enzymes. We do not know the level of expression or activity of COX and LOX enzymes in JCR rats, but studies in Zucker rats suggest that COX is either increased [83] or unchanged [84], while LOX is decreased [85], hypothetically resulting in no major net change in AA consumption. Moreover, our results in this study indicate that the increase in 20-HETE production is proportional to the increase in CYP4A and CYP4F expression. Taking this information together, we hypothesize that both AA production and CYP4A/4F expression/activity are increased in JCR rats, but that the actual amount of 20-HETE produced is regulated by CYP4A/4F expression levels.

20-HETE enhanced COX-derived vasoconstrictors were found in obese Zucker rats [86], and COX 1 but not COX 2 expression was increased, with accompanying increased vasoconstriction in aortic rings from rats fed a high fat diet [83]. In contrast, 73% reduction in PGI2 synthase but no change in COX was seen in coronary arteries of Zucker diabetic fatty (ZDF) vs. normal rats [84]. A study showed that arachidonic acid-mediated relaxation of small mesenteric arteries in ZDF rats was impaired due to reduced 12-lipoxygenase expression and activity [85]. In agreement with these studies, 14,15-EETs and 11,12-EETs were significantly decreased in our metabolic syndrome rats, but none of the EETs (14,15-EETs, 11,12-EETs, 8,9-EETs or 5,6-EETs) were altered by 20-HETE antagonists further supporting the conclusion that 20-HETE is a major regulator of large artery compliance and systolic blood pressure in metabolic syndrome animals.

JCR rats, like other hypertensive models, exhibit VSM hypertrophy in large arteries. However, we have also previously shown that VSMCs in JCR rats, as in other metabolic syndrome and obese rat models, tend towards a more synthetic (vs. contractile) phenotype[87]. Thus, whether Ca^{2+}-dependent VSMC contraction is increased in JCR rats, as shown for other hypertensive rat models, is unknown. Since arterial stiffness and peripheral resistance, and therefore blood pressure, depend on these components, their respective 20-HETE and/or Ang II-sensitivity in metabolic syndrome is a subject of future studies and may further elucidate the systolic blood pressure-specific effect of the 20-HETE antagonists.

Our results further demonstrate that activation of MMP12 is markedly increased in the large arteries of metabolic syndrome vs. normal animals. MMP12, along with MMP2, MMP3, MMP7 and MMP9, is one of the MMPs capable of degrading elastin. In fact, elastin is the main substrate for MMP12 [88]. Unlike 20-HETE antagonists, which completely inhibited elastin degradation in JCR rats, inhibition of MMP12 resulted in significant but incomplete inhibition of elastin degradation indicating that MMP12 is not the only protease responsible for elastin degradation in metabolic syndrome. Similarly, MMP12 inhibition resulted in significant but incomplete reversal of arterial stiffness and systolic blood pressure in JCR rats. Similar results were seen in MMP12 −/− mice with respect to arterial stiffening in response to vascular (wire) injury [5].

Other MMPs, namely MMP2 and MMP9 have been implicated in the regulation of arterial stiffness. Increased serum MMP9 levels were correlated with increased arterial stiffness and isolated systolic hypertension in humans [89]. Inhibition of MMP2 and MMP9 activity in normal, healthy mice decreased arterial stiffness [10]. In our study, MMP2, MMP9, MMP3 or MMP7 are not involved in 20-HETE-dependent regulation of elastin degradation or regulation of arterial stiffness. This is consistent with our previous observations that activation of these MMPs is decreased in arteries from metabolic syndrome animals [90,48]. However, other elastases, for example cathepsin G from neutrophils, may play a role in elastin degradation.

Alternatively, elevated 20-HETE may block activation of signaling pathways needed to synthesize elastin. Our results demonstrate that in addition to increased degradation of elastin, total elastin content is decreased in metabolic syndrome suggesting a decrease in

elastin synthesis. In contrast, in addition to inhibiting its degradation, 20-HETE antagonists appear to promote elastin synthesis. In this study, we did not identify which cells might contribute to this new elastin synthesis, but hypothesize that they might be VSMCs. As mentioned above, VSMCs in JCR rats, as in other metabolic syndrome and obese rat models, tend towards a more synthetic (vs. contractile) phenotype [87], which correlates with a shift in extracellular matrix production from elastin and laminin towards type III collagen, as shown in this study, and osteopontin as demonstrated previously [79]. Our preliminary observations suggest that 20-HETE antagonists may restore the contractile VSMC phenotype (Rocic and Schawartzman, unpublished data, 2017).

Upstream regulators of MMP12 remain largely unknown. TIMPs do not appear to regulate 20-HETE-dependent MMP12 activation. It is possible that 20-HETE antagonists inhibit activation of upstream regulators of MMP12 activation. p38 and JNK MAP kinases and PI3-kinase have been shown to be involved in MMP12 activation in airway smooth muscle [91]. These signaling intermediates are also known to be activated by 20-HETE in various cell types [92–94].

Thus, we believe that MMP12 activity is regulated by neither its expression levels, which are stable between phenotypes and in response to 20-HETE antagonists, nor by TIMPS, but by an upstream protease(s), which cleaves the pro-form into the active form. The identity of this upstream regulator is the subject of ongoing studies.

Another limitation of the present study is that we did not identify the cellular source of MMP12. However, macrophages and neutrophils have been identified as its major sources across several tissues and pathologies [95]. On the other hand, a single study reported MMP12 production from synthetic VSMCs [5]. The arterial vasculature of metabolic syndrome animal models and humans has been described to contain pre-atherosclerotic lesions containing macrophages in humans and neutrophils in rats [22,23]. Specifically, existence of neointimal lesions at 10+ weeks of age has been described in JCR rats [22,23]. We have recently reported a significant increase in neutrophils in JCR rats [80]. Whether or not neutrophils (or possibly macrophages) are indeed the source of MMP12 and how neutrophils and other inflammatory cells interplay with 20-HETE signaling to regulate arterial stiffness and systolic blood pressure will be the subject of our future studies.

Supplementary Material

Refer to Web version on PubMed Central for supplementary material.

Acknowledgments

The authors would like to acknowledge Dr. Alberto Nasjletti (Department of Pharmacology, New York Medical College) for critical review of the manuscript prior to submission.

SOURCES OF FUNDING

NIH R01HL093052 (PR), NIH 1F31HL137356 (AS), P01HL034300 (MLS)

References

1. Mitchell GF. Arterial stiffness and hypertension: chicken or egg? Hypertension. 2014; 64:210–4. [PubMed: 24799614]
2. Lemarié CA, Tharaux P-L, Lehoux S. Extracellular matrix alterations in hypertensive vascular remodeling. J Mol Cell Cardiol. 2010; 48:433–9. [PubMed: 19837080]
3. Wagenseil JE, Mecham RP. Elastin in large artery stiffness and hypertension. J Cardiovasc Transl Res. 2012; 5:264–73. [PubMed: 22290157]
4. Fulcher YG, Van Doren SR. Remote exosites of the catalytic domain of matrix metalloproteinase-12 enhance elastin degradation. Biochemistry. 2011; 50:9488–99. [PubMed: 21967233]
5. Liu S-L, Bae YH, Yu C, Monslow J, Hawthorne EA, Castagnino P, et al. Matrix metalloproteinase-12 is an essential mediator of acute and chronic arterial stiffening. Sci Rep. 2015; 5:17189. [PubMed: 26608672]
6. Houghton AM. Matrix metalloproteinases in destructive lung disease. Matrix Biol. 2015; 44–46:167–74.
7. Goncalves I, Bengtsson E, Colhoun HM, Shore AC, Palombo C, Natali A, et al. Elevated Plasma Levels of MMP-12 Are Associated With Atherosclerotic Burden and Symptomatic Cardiovascular Disease in Subjects With Type 2 Diabetes. Arterioscler Thromb Vasc Biol. 2015; 35:1723–31. [PubMed: 25953645]
8. Curci JA, Liao S, Huffman MD, Shapiro SD, Thompson RW. Expression and localization of macrophage elastase (matrix metalloproteinase-12) in abdominal aortic aneurysms. J Clin Invest. 1998; 102:1900–10. [PubMed: 9835614]
9. Lv F-Z, Wang J-L, Wu Y, Chen H-F, Shen X-Y. Knockdown of MMP12 inhibits the growth and invasion of lung adenocarcinoma cells. Int J Immunopathol Pharmacol. 2015; 28:77–84. [PubMed: 25816409]
10. Anea CB, Ali MI, Osmond JM, Sullivan JC, Stepp DW, Merloiu AM, et al. Matrix metalloproteinase 2 and 9 dysfunction underlie vascular stiffness in circadian clock mutant mice. Arterioscler Thromb Vasc Biol. 2010; 30:2535–43. [PubMed: 20829506]
11. Wu C-C, Gupta T, Garcia V, Ding Y, Schwartzman ML. 20-HETE and Blood Pressure Regulation. Cardiol Rev. 2014; 22:1–12. [PubMed: 23584425]
12. Gebremedhin D, Lange AR, Narayanan J, Aebly MR, Jacobs ER, Harder DR. Cat cerebral arterial smooth muscle cells express cytochrome P450 4A2 enzyme and produce the vasoconstrictor 20-HETE which enhances L-type Ca2+ current. J Physiol. 1998; 507(Pt 3):771–81. [PubMed: 9508838]
13. Tsai IJ, Croft KD, Puddey IB, Beilin LJ, Barden A. 20-Hydroxyeicosatetraenoic acid synthesis is increased in human neutrophils and platelets by angiotensin II and endothelin-1. Am J Physiol Heart Circ Physiol. 2011; 300:H1194–200. [PubMed: 21239640]
14. Abraham NG, Feldman E, Falck JR, Lutton JD, Schwartzman ML. Modulation of erythropoiesis by novel human bone marrow cytochrome P450-dependent metabolites of arachidonic acid. Blood. 1991; 78:1461–6. [PubMed: 1909194]
15. Sacerdoti D, Escalante B, Abraham NG, McGiff JC, Levere RD, Schwartzman ML. Treatment with tin prevents the development of hypertension in spontaneously hypertensive rats. Science. 1989; 243:388–90. [PubMed: 2492116]
16. Muller DN, Schmidt C, Barbosa-Sicard E, Wellner M, Gross V, Hercule H, et al. Mouse Cyp4a isoforms: enzymatic properties, gender- and strain-specific expression, and role in renal 20-hydroxyeicosatetraenoic acid formation. Biochem J. 2007; 403:109–18. [PubMed: 17112342]
17. Inoue K, Sodhi K, Puri N, Gotlinger KH, Cao J, Rezzani R, et al. Endothelial-specific CYP4A2 overexpression leads to renal injury and hypertension via increased production of 20-HETE. Am J Physiol Renal Physiol. 2009; 297:F875–84. [PubMed: 19675180]
18. Singh H, Cheng J, Deng H, Kemp R, Ishizuka T, Nasjletti A, et al. Vascular cytochrome P450 4A expression and 20-hydroxyeicosatetraenoic acid synthesis contribute to endothelial dysfunction in androgen-induced hypertension. Hypertension. 2007; 50:123–9. [PubMed: 17548721]

19. Wu C-C, Mei S, Cheng J, Ding Y, Weidenhammer A, Garcia V, et al. Androgen-sensitive hypertension associates with upregulated vascular CYP4A12-20-HETE synthase. J Am Soc Nephrol. 2013; 24:1288–96. [PubMed: 23641057]

20. Garcia V, Joseph G, Shkolnik B, Ding Y, Zhang FF, Gotlinger K, et al. Angiotensin II receptor blockade or deletion of vascular endothelial ACE does not prevent vascular dysfunction and remodeling in 20-HETE-dependent hypertension. Am J Physiol Regul Integr Comp Physiol. 2015; 309:R71–8. [PubMed: 25924878]

21. Hunter I, Soler A, Joseph G, Hutcheson B, Bradford C, Zhang FF, et al. Cardiovascular function in male and female JCR:LA-cp rats: effect of high-fat/high-sucrose diet. Am J Physiol - Hear Circ Physiol. 2017; 312:H742–H751.

22. Liao J, Huang W, Liu G. Animal models of coronary heart disease. J Biomed Res. 2015; :30.doi: 10.7555/JBR.30.20150051

23. Reimer RA, Russell JC. Glucose tolerance, lipids, and GLP-1 secretion in JCR:LA-cp rats fed a high protein fiber diet. Obesity (Silver Spring). 2008; 16:40–6. [PubMed: 18223610]

24. Gangadhariah MH, Luther JM, Garcia V, Paueksakon P, Zhang M-Z, Hayward SW, et al. Hypertension is a major contributor to 20-hydroxyeicosatetraenoic acid-mediated kidney injury in diabetic nephropathy. J Am Soc Nephrol. 2015; 26:597–610. [PubMed: 25071086]

25. Dodd TY, Wiggins L, Musiyenko A, Smith E, Rocic P. Increased MMP8 and 12 activation correlates with elevated endostatin and angiostatin and impaired coronary collateral growth in the metabolic syndrome. FASEB J. 2012; 26:1060.11.

26. Hattan N, Chilian WM, Park F, Rocic P. Restoration of coronary collateral growth in the Zucker obese rat: impact of VEGF and ecSOD. Basic Res Cardiol. 2007; 102:217–23. [PubMed: 17323199]

27. Park F, Ohashi K, Kay MA. Therapeutic levels of human factor VIII and IX using HIV-1-based lentiviral vectors in mouse liver. Blood. 2000; 96:1173–6. [PubMed: 10910939]

28. Cheng J, Garcia V, Ding Y, Wu C-C, Thakar K, Falck JR, et al. Induction of angiotensin-converting enzyme and activation of the renin-angiotensin system contribute to 20-hydroxyeicosatetraenoic acid-mediated endothelial dysfunction. Arterioscler Thromb Vasc Biol. 2012; 32:1917–24. [PubMed: 22723444]

29. Wu C-C, Cheng J, Zhang FF, Gotlinger KH, Kelkar M, Zhang Y, et al. Androgen-dependent hypertension is mediated by 20-hydroxy-5,8,11,14-eicosatetraenoic acid-induced vascular dysfunction: role of inhibitor of kappaB Kinase. Hypertension. 2011; 57:788–94. [PubMed: 21321301]

30. Toyota E, Warltier DC, Brock T, Ritman E, Kolz C, O'Malley P, et al. Vascular endothelial growth factor is required for coronary collateral growth in the rat. Circulation. 2005; 112:2108–13. [PubMed: 16203926]

31. Reed R, Potter B, Smith E, Jadhav R, Villalta P, Jo H, et al. Redox-sensitive Akt and Src regulate coronary collateral growth in metabolic syndrome. AJP Hear Circ Physiol. 2009; 296:H1811–H1821.

32. Xu F, Falck JR, Ortiz de Montellano PR, Kroetz DL. Catalytic activity and isoform-specific inhibition of rat cytochrome p450 4F enzymes. J Pharmacol Exp Ther. 2004; 308:887–95. [PubMed: 14634044]

33. Marji JS, Wang M-H, Laniado-Schwartzman M. Cytochrome *P*-450 4A isoform expression and 20-HETE synthesis in renal preglomerular arteries. Am J Physiol - Ren Physiol. 2002; 283:F60–F67.

34. Kikuta Y, Yamashita Y, Kashiwagi S, Tani K, Okada K, Nakata K. Expression and induction of CYP4F subfamily in human leukocytes and HL60 cells. Biochim Biophys Acta - Mol Cell Biol Lipids. 2004; 1683:7–15.

35. Joseph G, Soler A, Hutcheson R, Hunter I, Bradford C, Hutcheson B, et al. Elevated 20-HETE impairs coronary collateral growth in metabolic syndrome via endothelial dysfunction. Am J Physiol - Hear Circ Physiol. 2017; 312:H528–H540.

36. Orozco LD, Liu H, Perkins E, Johnson DA, Chen BB, Fan F, et al. 20-Hydroxyeicosatetraenoic Acid Inhibition Attenuates Balloon Injury-Induced Neointima Formation and Vascular

Remodeling in Rat Carotid Arteries. J Pharmacol Exp Ther. 2013; 346:67–74. [PubMed: 23658377]

37. Imig JD. Epoxides and soluble epoxide hydrolase in cardiovascular physiology. Physiol Rev. 2012; 92:101–30. [PubMed: 22298653]
38. Pandey V, Garcia V, Gilani A, Mishra P, Zhang FF, Paudyal MP, et al. The Blood Pressure-Lowering Effect of 20-HETE Blockade in Cyp4a14(−/−) Mice Is Associated with Natriuresis. J Pharmacol Exp Ther. 2017; 363:412–418. [PubMed: 28912346]
39. Garcia V, Joseph G, Shkolnik B, Ding Y, Zhang FF, Gotlinger K, et al. Angiotensin II receptor blockade or deletion of vascular endothelial ACE does not prevent vascular dysfunction and remodeling in 20-HETE-dependent hypertension. Am J Physiol Regul Integr Comp Physiol. 2015; 309:R71–8. [PubMed: 25924878]
40. Kappert K, Meyborg H, Baumann B, Furundzija V, Kaufmann J, Graf K, et al. Integrin cleavage facilitates cell surface-associated proteolysis required for vascular smooth muscle cell invasion. Int J Biochem Cell Biol. 2009; 41:1511–1517. [PubMed: 19166965]
41. Kim Y, Remacle AG, Chernov AV, Liu H, Shubayev I, Lai C, et al. The MMP-9/TIMP-1 Axis Controls the Status of Differentiation and Function of Myelin-Forming Schwann Cells in Nerve Regeneration. PLoS One. 2012; 7:e33664. [PubMed: 22438979]
42. Sasamura H, Kitamura Y, Nakamura M, Ryuzaki M, Saruta T. Effects of the Angiotensin Receptor Blocker Candesartan on Arterial Stiffness and Markers of Extracellular Matrix Metabolism in Patients with Essential Hypertension. Clin Exp Hypertens. 2006; 28:511–520. [PubMed: 16820347]
43. Stöhr R, Kappel BA, Carnevale D, Cavalera M, Mavilio M, Arisi I, et al. TIMP3 interplays with apelin to regulate cardiovascular metabolism in hypercholesterolemic mice. Mol Metab. 2015; 4:741–752. [PubMed: 26500845]
44. Berillis P. The Role of Collagen in the Aorta's Structure. 2013; 6:1–8.
45. El Mabrouk M, Touyz RM, Schiffrin EL. Differential ANG II-induced growth activation pathways in mesenteric artery smooth muscle cells from SHR. Am J Physiol Heart Circ Physiol. 2001; 281:H30–9. [PubMed: 11406465]
46. Sabri A, Levy BI, Poitevin P, Caputo L, Faggin E, Marotte F, et al. Differential roles of AT1 and AT2 receptor subtypes in vascular trophic and phenotypic changes in response to stimulation with angiotensin II. Arterioscler Thromb Vasc Biol. 1997; 17:257–64. [PubMed: 9081679]
47. Zafari AM, Ushio-Fukai M, Akers M, Yin Q, Shah A, Harrison DG, et al. Role of NADH/NADPH oxidase-derived H2O2 in angiotensin II-induced vascular hypertrophy. Hypertens (Dallas, Tex 1979). 1998; 32:488–95.
48. Dodd T, Wiggins L, Hutcheson R, Smith E, Musiyenko A, Hysell B, et al. Impaired coronary collateral growth in the metabolic syndrome is in part mediated by matrix metalloproteinase 12-dependent production of endostatin and angiostatin. Arterioscler Thromb Vasc Biol. 2013; 33:1339–49. [PubMed: 23599440]
49. Smith ER, Tomlinson LA, Ford ML, McMahon LP, Rajkumar C, Holt SG. Elastin degradation is associated with progressive aortic stiffening and all-cause mortality in predialysis chronic kidney disease. Hypertension. 2012; 59:973–8. [PubMed: 22411928]
50. Liao S, Miralles M, Kelley BJ, Curci JA, Borhani M, Thompson RW. Suppression of experimental abdominal aortic aneurysms in the rat by treatment with angiotensin-converting enzyme inhibitors. J Vasc Surg. 2001; 33:1057–64. [PubMed: 11331849]
51. Salum E, Butlin M, Kals J, Zilmer M, Eha J, Avolio AP, et al. Angiotensin II receptor blocker telmisartan attenuates aortic stiffening and remodelling in STZ-diabetic rats. Diabetol Metab Syndr. 2014; 6:57. [PubMed: 24920962]
52. Intengan HD, Thibault G, Li JS, Schiffrin EL. Resistance artery mechanics, structure, and extracellular components in spontaneously hypertensive rats: effects of angiotensin receptor antagonism and converting enzyme inhibition. Circulation. 1999; 100:2267–75. [PubMed: 10578002]
53. Levy BI, Michel JB, Salzmann JL, Azizi M, Poitevin P, Safar M, et al. Effects of chronic inhibition of converting enzyme on mechanical and structural properties of arteries in rat renovascular hypertension. Circ Res. 1988; 63:227–39. [PubMed: 3383377]

54. Michel JB, Heudes D, Michel O, Poitevin P, Philippe M, Scalbert E, et al. Effect of chronic ANG I-converting enzyme inhibition on aging processes. II. Large arteries. Am J Physiol. 1994; 267:R124–35. [PubMed: 8048614]
55. Ng K, Butlin M, Avolio AP. Persistent effect of early, brief angiotensin-converting enzyme inhibition on segmental pressure dependency of aortic stiffness in spontaneously hypertensive rats. J Hypertens. 2012; 30:1782–90. [PubMed: 22759780]
56. Chamiot Clerc P, Renaud JF, Blacher J, Legrand M, Samuel JL, Levy BI, et al. Collagen I and III and mechanical properties of conduit arteries in rats with genetic hypertension. J Vasc Res. 36:139–46.
57. Bashey RI, Cox R, McCann J, Jimenez SA. Changes in collagen biosynthesis, types, and mechanics of aorta in hypertensive rats. J Lab Clin Med. 1989; 113:604–11. [PubMed: 2715682]
58. McNulty M, Mahmud A, Spiers P, Feely J. Collagen type-I degradation is related to arterial stiffness in hypertensive and normotensive subjects. J Hum Hypertens. 2006; 20:867–873. [PubMed: 16598292]
59. Prenner SB, Chirinos JA. Arterial stiffness in diabetes mellitus. Atherosclerosis. 2015; 238:370–379. [PubMed: 25558032]
60. Muthalif MM, Benter IF, Karzoun N, Fatima S, Harper J, Uddin MR, et al. 20-Hydroxyeicosatetraenoic acid mediates calcium/calmodulin-dependent protein kinase II-induced mitogen-activated protein kinase activation in vascular smooth muscle cells. Proc Natl Acad Sci U S A. 1998; 95:12701–6. [PubMed: 9770549]
61. Amaral SL, Maier KG, Schippers DN, Roman RJ, Greene AS. CYP4A metabolites of arachidonic acid and VEGF are mediators of skeletal muscle angiogenesis. Am J Physiol Heart Circ Physiol. 2003; 284:H1528–35. [PubMed: 12521947]
62. Imig JD, Zou AP, Stec DE, Harder DR, Falck JR, Roman RJ. Formation and actions of 20-hydroxyeicosatetraenoic acid in rat renal arterioles. Am J Physiol. 1996; 270:R217–27. [PubMed: 8769805]
63. Jiang M, Mezentsev A, Kemp R, Byun K, Falck JR, Miano JM, et al. Smooth muscle--specific expression of CYP4A1 induces endothelial sprouting in renal arterial microvessels. Circ Res. 2004; 94:167–74. [PubMed: 14670847]
64. Williams JM, Murphy S, Burke M, Roman RJ. 20-hydroxyeicosatetraeonic acid: a new target for the treatment of hypertension. J Cardiovasc Pharmacol. 2010; 56:336–44. [PubMed: 20930591]
65. Sodhi K, Wu C-C, Cheng J, Gotlinger K, Inoue K, Goli M, et al. CYP4A2-induced hypertension is 20-hydroxyeicosatetraenoic acid- and angiotensin II-dependent. Hypertension. 2010; 56:871–8. [PubMed: 20837888]
66. Alonso-Galicia M, Maier KG, Greene AS, Cowley AW, Roman RJ. Role of 20-hydroxyeicosatetraenoic acid in the renal and vasoconstrictor actions of angiotensin II. Am J Physiol Regul Integr Comp Physiol. 2002; 283:R60–8. [PubMed: 12069931]
67. Carroll MA, Balazy M, Huang DD, Rybalova S, Falck JR, McGiff JC. Cytochrome P450-derived renal HETEs: storage and release. Kidney Int. 1997; 51:1696–702. [PubMed: 9186856]
68. Croft KD, McGiff JC, Sanchez-Mendoza A, Carroll MA. Angiotensin II releases 20-HETE from rat renal microvessels. Am J Physiol Renal Physiol. 2000; 279:F544–51. [PubMed: 10966934]
69. Chábová VC, Kramer HJ, Vanecková I, Vernerová Z, Eis V, Tesar V, et al. Effects of chronic cytochrome P-450 inhibition on the course of hypertension and end-organ damage in Ren-2 transgenic rats. Vascul Pharmacol. 47:145–59.
70. Hoopes SL, Garcia V, Edin ML, Schwartzman ML, Zeldin DC. Vascular actions of 20-HETE. Prostaglandins Other Lipid Mediat. 2015; 120:9–16. [PubMed: 25813407]
71. Fan F, Muroya Y, Roman RJ. Cytochrome P450 eicosanoids in hypertension and renal disease. Curr Opin Nephrol Hypertens. 2015; 24:37–46. [PubMed: 25427230]
72. Vasudevan H, Yuen VG, McNeill JH. Testosterone-dependent increase in blood pressure is mediated by elevated Cyp4A expression in fructose-fed rats. Mol Cell Biochem. 2012; 359:409–18. [PubMed: 21894443]
73. Tsai I-J, Croft KD, Mori TA, Falck JR, Beilin LJ, Puddey IB, et al. 20-HETE and F2-isoprostanes in the metabolic syndrome: the effect of weight reduction. Free Radic Biol Med. 2009; 46:263–70. [PubMed: 19013235]

74. Theken KN, Deng Y, Schuck RN, Oni-Orisan A, Miller TM, Kannon MA, et al. Enalapril reverses high-fat diet-induced alterations in cytochrome P450-mediated eicosanoid metabolism. Am J Physiol Endocrinol Metab. 2012; 302:E500–9. [PubMed: 22185841]

75. Croft KD, McGiff JC, Sanchez-Mendoza A, Carroll MA. Angiotensin II releases 20-HETE from rat renal microvessels. Am J Physiol Physiol. 2000; 279:F544–F551.

76. Joseph G, Soler A, Hutcheson R, Hunter I, Bradford C, Hutcheson B, et al. Elevated 20-HETE impairs coronary collateral growth in metabolic syndrome via endothelial dysfunction. Am J Physiol Heart Circ Physiol. 2017; 312:H528–H540. [PubMed: 28011587]

77. Alonso-Galicia M, Drummond HA, Reddy KK, Falck JR, Roman RJ. Inhibition of 20-HETE production contributes to the vascular responses to nitric oxide. Hypertens (Dallas, Tex 1979). 1997; 29:320–5.

78. Cheng J, Ou J-S, Singh H, Falck JR, Narsimhaswamy D, Pritchard KA, et al. 20-Hydroxyeicosatetraenoic acid causes endothelial dysfunction via eNOS uncoupling. AJP Hear Circ Physiol. 2007; 294:H1018–H1026.

79. Hutcheson R, Chaplin J, Hutcheson B, Borthwick F, Proctor S, Gebb S, et al. miR-21 normalizes vascular smooth muscle proliferation and improves coronary collateral growth in metabolic syndrome. FASEB J. 2014; 28:4088–99. [PubMed: 24903275]

80. Hutcheson R, Terry R, Hutcheson B, Jadhav R, Chaplin J, Smith E, et al. miR-21-mediated decreased neutrophil apoptosis is a determinant of impaired coronary collateral growth in metabolic syndrome. Am J Physiol - Hear Circ Physiol. 2015; 308:H1323–H1335.

81. Acevedo M, Varleta P, Kramer V, Valentino G, Quiroga T, Prieto C, et al. Comparison of Lipoprotein-Associated Phospholipase A2 and High Sensitive C-Reactive Protein as Determinants of Metabolic Syndrome in Subjects without Coronary Heart Disease: In Search of the Best Predictor. Int J Endocrinol. 2015; 2015:934681. [PubMed: 26089902]

82. Tsimikas S, Willeit J, Knoflach M, Mayr M, Egger G, Notdurfter M, et al. Lipoprotein-associated phospholipase A2 activity, ferritin levels, metabolic syndrome, and 10-year cardiovascular and non-cardiovascular mortality: results from the Bruneck study. Eur Heart J. 2008; 30:107–115. [PubMed: 19019993]

83. Smith AD, Dorrance AM. Arachidonic acid induces augmented vasoconstriction via cyclooxygenase 1 in the aorta from rats fed a high-fat diet. Prostaglandins, Leukot Essent Fat Acids. 2006; 75:43–49.

84. Lu T, Wang X-L, He T, Zhou W, Kaduce TL, Katusic ZS, et al. Impaired arachidonic acid-mediated activation of large-conductance Ca2+-activated K+ channels in coronary arterial smooth muscle cells in Zucker Diabetic Fatty rats. Diabetes. 2005; 54:2155–63. [PubMed: 15983217]

85. Zhou, W., Wang, X-L., Kaduce, TL., Spector, AA., Lee, H-C. [accessed 9 Jun 2017] Impaired arachidonic acid-mediated dilation of small mesenteric arteries in Zucker diabetic fatty rats; Am J Physiol - Hear Circ Physiol. 2005. p. 288http://ajpheart.physiology.org/content/288/5/H2210

86. Mingorance C, Alvarez de Sotomayor M, Jiménez-Palacios FJ, Callejón Mochón M, Casto C, Marhuenda E, et al. Effects of Chronic Treatment With the CB1 Antagonist, Rimonabant on the Blood Pressure, and Vascular Reactivity of Obese Zucker Rats. Obesity. 2009; 17:1340–7. [PubMed: 19553924]

87. Hutcheson R, Terry R, Chaplin J, Smith E, Musiyenko A, Russell JC, et al. MicroRNA-145 restores contractile vascular smooth muscle phenotype and coronary collateral growth in the metabolic syndrome. Arterioscler Thromb Vasc Biol. 2013; 33:727–36. [PubMed: 23393394]

88. Ford ES, Giles WH, Mokdad AH. Increasing prevalence of the metabolic syndrome among u.s. Adults. Diabetes Care. 2004; 27:2444–9. [PubMed: 15451914]

89. Yasmin, McEniery CM, Wallace S, Dakham Z, Pulsalkar P, Pusalkar P, et al. Matrix metalloproteinase-9 (MMP-9), MMP-2, and serum elastase activity are associated with systolic hypertension and arterial stiffness. Arterioscler Thromb Vasc Biol. 2005; 25:372. [PubMed: 15556929]

90. Dodd T, Jadhav R, Wiggins L, Stewart J, Smith E, Russell JC, et al. MMPs 2 and 9 are essential for coronary collateral growth and are prominently regulated by p38 MAPK. J Mol Cell Cardiol. 2011; 51:1015–1025. [PubMed: 21884701]

91. Xie S, Issa R, Sukkar MB, Oltmanns U, Bhavsar PK, Papi A, et al. Induction and regulation of matrix metalloproteinase-12in human airway smooth muscle cells. Respir Res. 2005; 6:148. [PubMed: 16359550]

92. Kalyankrishna S, Malik KU. Norepinephrine-Induced Stimulation of p38 Mitogen-Activated Protein Kinase Is Mediated by Arachidonic Acid Metabolites Generated by Activation of Cytosolic Phospholipase A 2 in Vascular Smooth Muscle Cells.

93. Liu Y, Wang D, Wang H, Qu Y, Xiao X, Zhu Y. The protective effect of HET0016 on brain edema and blood–brain barrier dysfunction after cerebral ischemia/reperfusion. Brain Res. 2014; 1544:45–53. [PubMed: 24316243]

94. Bodiga S, Gruenloh SK, Gao Y, Manthati VL, Dubasi N, Falck JR, et al. 20-HETE-induced nitric oxide production in pulmonary artery endothelial cells is mediated by NADPH oxidase, H2O2, and PI3-kinase/Akt. Am J Physiol Lung Cell Mol Physiol. 2010; 298:L564–74. [PubMed: 20061439]

95. Lee J-T, Pamir N, Liu N-C, Kirk EA, Averill MM, Becker L, et al. Macrophage metalloelastase (MMP12) regulates adipose tissue expansion, insulin sensitivity, and expression of inducible nitric oxide synthase. Endocrinology. 2014; 155:3409–20. [PubMed: 24914938]

Highlights

- 20-HETE regulates large artery remodeling (arterial stiffness) via MMP12 activation and elastin degradation
- 20-HETE antagonists reverse arterial stiffness and normalize systolic blood pressure in metabolic syndrome
- Effects of 20-HETE antagonists on arterial stiffness are angiotensin II (Ang II)-independent and their effects on systolic blood pressure are only partially Ang II-dependent
- 20-HETE antagonists may provide viable therapy for treatment of isolated systolic hypertension

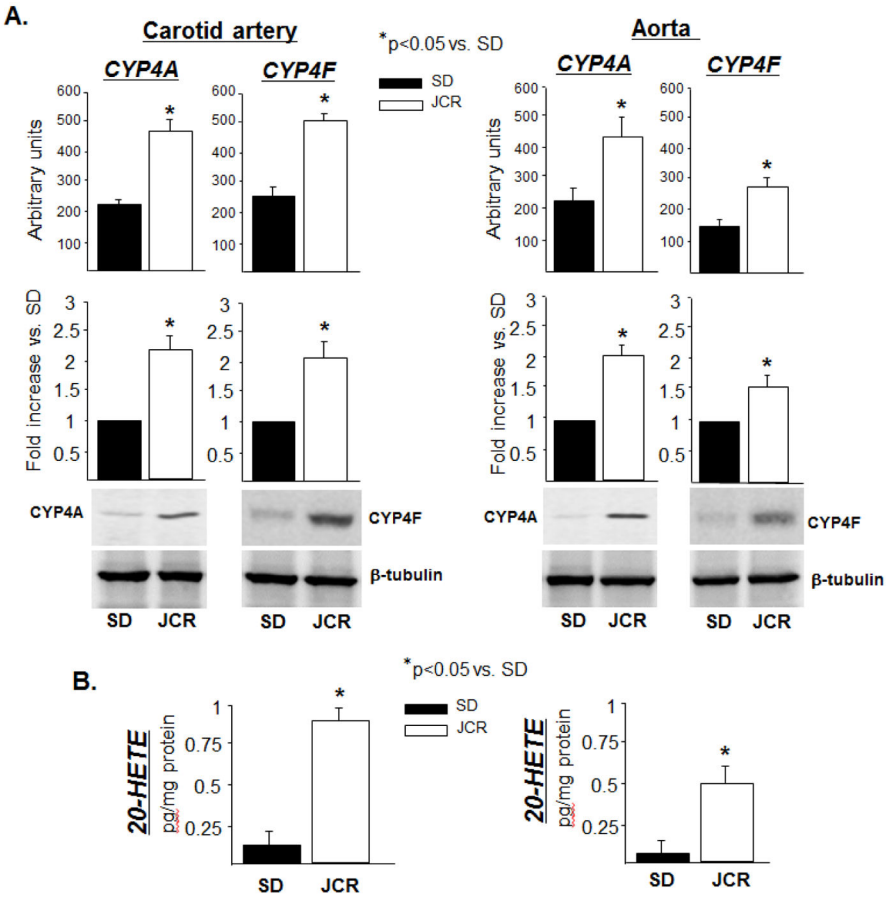

FIGURE 1.

SD and JCR rats were sacrificed and arterial tissue collected. **A.** Representative Western blots (bottom) and cumulative data (top) showing CYP4A and CYP4F expression in carotid artery and aorta tissue homogenates. **B.** LC-MS quantitation of 20-HETE production represented in pg/mg protein. n=8, * $p<0.05$ as indicated.

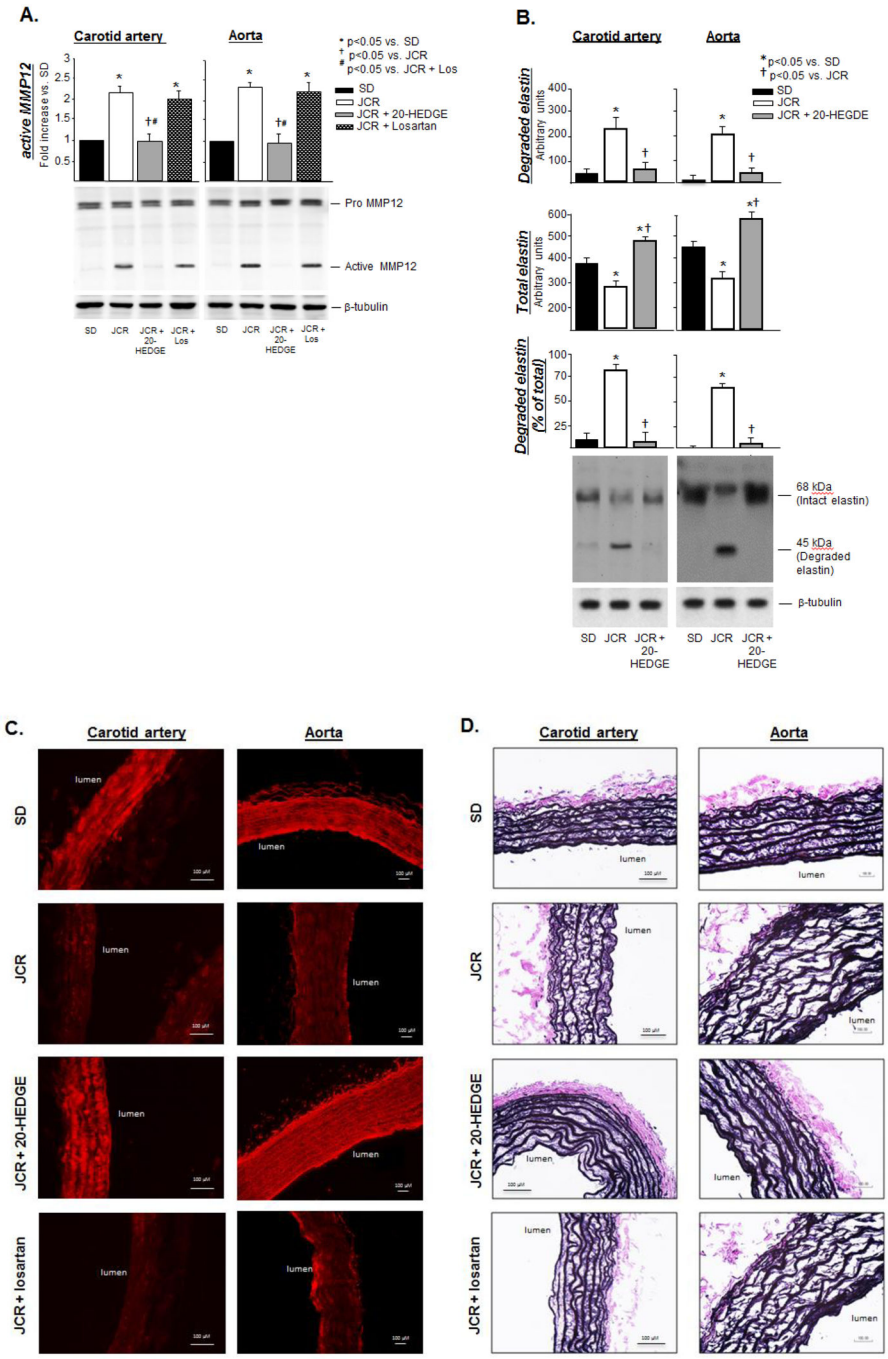

FIGURE 2.

SD and JCR rats were treated with 20-HEDGE or losartan for 14 days where indicated, sacrificed and arterial tissue collected. **A.** Representative Western blots (bottom) and cumulative data (top) showing pro and active (cumulative data) MMP12 expression (**A**) or total and degraded elastin (**B**) in carotid artery and aorta tissue homogenates are shown. Representative IHC (with anti-elastin antibodies which recognize only intact elastin, red) (**C**) and Verhoeff–Van Gieson (VVG, black) (**D**) staining of carotid artery and aorta tissue sections. n=8, *, †, # $p<0.05$ as indicated.

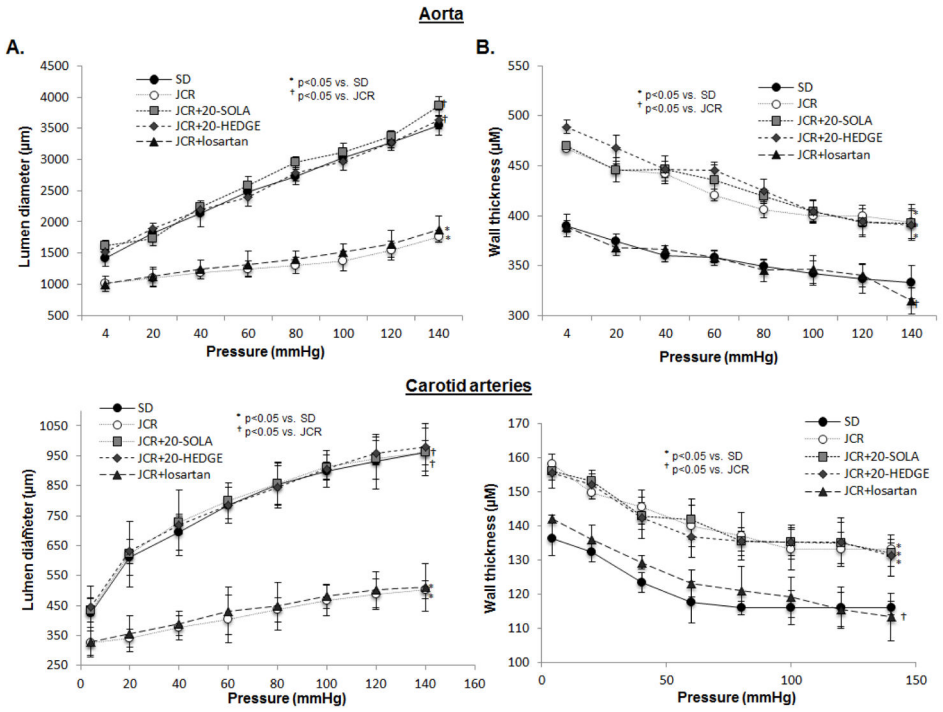

FIGURE 3.

JCR rats were treated with 20-HEDGE, 20-SOLA or losartan for 14 days where indicated. SD and JCR rats were sacrificed and carotid arteries and aorta collected. Lumen diameter (**A**) and wall thickness (**B**) were measured on a pressure myograph at increasing pressures 4–140 mmHg. n=8, *, † $p<0.05$ as indicated.

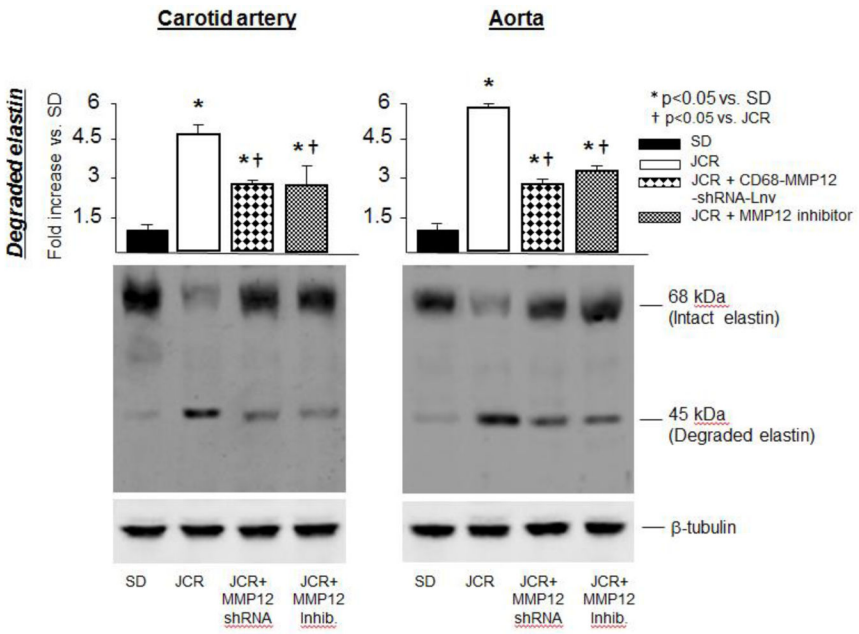

FIGURE 4.

SD and JCR rats were treated with the MMP12-shRNA-Lnv or the pharmacological MMP12 inhibitor for 14 days where indicated, sacrificed and arterial tissue collected. Representative Western blots (bottom) and cumulative data (top) showing total and degraded (cumulative data) elastin in carotid artery and aorta tissue homogenates are shown. n=8, *, † $p<0.05$ as indicated.

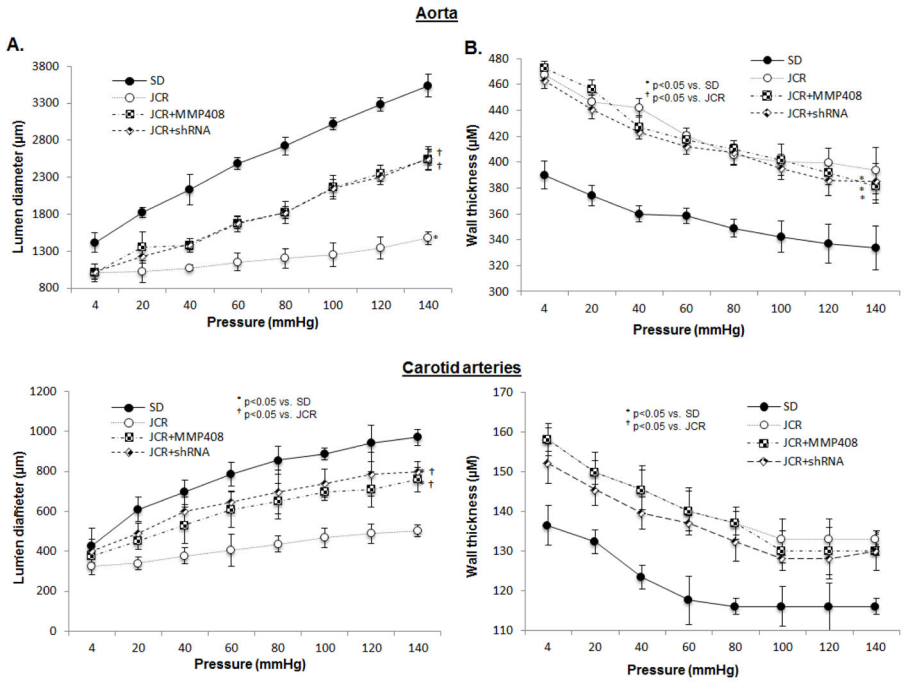

FIGURE 5.

JCR rats were treated with the MMP12-shRNA-Lnv or the pharmacological MMP12 inhibitor for 14 days where indicated. SD and JCR rats were sacrificed and carotid arteries and aorta collected. Lumen diameter (**A**) and wall thickness (**B**) were measured on a pressure myograph at increasing pressures 4–140 mmHg. n=8, *, † $p<0.05$ as indicated.

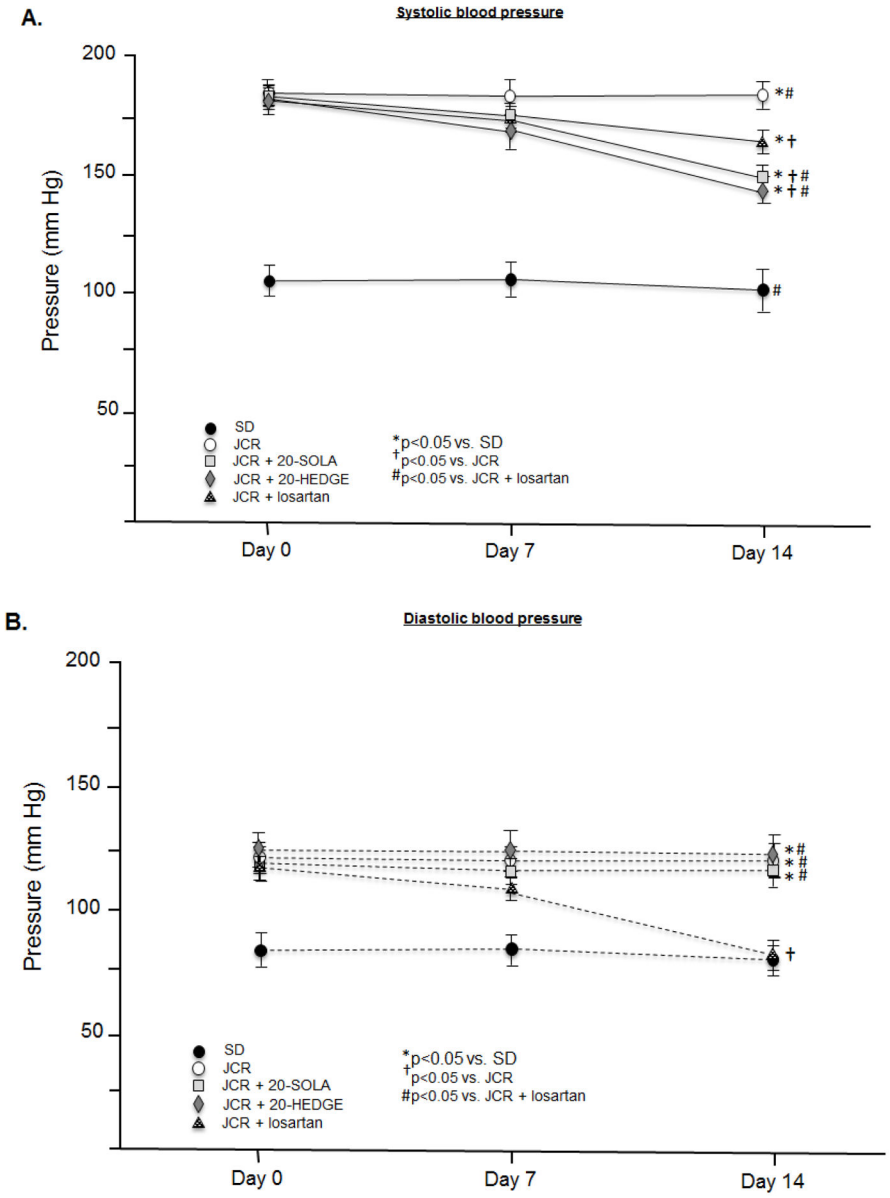

FIGURE 6.

JCR rats were treated with 20-HEDGE, 20-SOLA or losartan for 14 days where indicated. Systolic (**A**) and diastolic (**B**) blood pressure was measured in SD and JCR rats using an aortic catheter connected to a pressure transducer (Millar) on day 0, 7 and 14 of treatment. n=8, *, †, # $p<0.05$ as indicated.